

Timing with resonant gravitational wave detectors: An experimental test

V. Crivelli-Visconti, A. Ortolan, L. Taffarelo, and G. Vedovato
INFN, Laboratori Nazionali di Legnaro, via Romea 4, I-35020, Legnaro, Padova, Italy

M. Cerdonio
Dipartimento di Fisica, Università di Padova and INFN, Sezione di Padova, via Marzolo, 8 35100 Padova, Italy

G. A. Prodi and S. Vitale
Dipartimento di Fisica, Università di Trento and INFN, Gruppo Collegato di Trento, Sezione di Padova, I-38050, Povo, Trento, Italy
 (Received 27 May 1997; published 23 January 1998)

We measure the time of arrival t_0 of a force signal acting on a room temperature gravitational wave antenna. The antenna has a noise spectral density whose shape is a rescaled replica of that predicted for the two subkelvin antennas located in Italy, once at their sensitivity goal. t_0 is expressed as $t_0 = t_\phi + kT_0$ where T_0 is half the natural period of oscillation of the antenna, $|t_\phi| \leq T_0/2$, and k is an integer. We measure the phase part t_ϕ with an accuracy of $\sigma_{t_\phi} \approx 174 \mu\text{s}/\text{SNR}$, where SNR is the signal to noise ratio for the signal amplitude. We also find that, for $\text{SNR} \geq 20$, the error on k is $\delta k \ll 1$ so that the total statistical error on the arrival time reduces to the phase error σ_{t_ϕ} . We discuss how this last result can be achieved even for smaller values of the SNR, by better tuning the modes of the antenna. We finally discuss the relevance of these results for source location and spurious events rejection with the two subkelvin detectors above. [S0556-2821(98)03404-3]

PACS number(s): 04.80.Nn, 95.55.Ym

I. INTRODUCTION

Two subkelvin ($T \approx 50$ mK), resonant (≈ 1 kHz) gravitational wave antennae aimed at a burst sensitivity of $h_{\min} \cong 3 \times 10^{-20}$ and a post-detection bandwidth of ≈ 50 Hz [1] have been built in Italy [2], and they are going to operate in coincidence in the near future.

The experiment's target is to detect bursts from supernova explosions or from coalescence of binary neutron star systems. For these kinds of signals, the relatively large bandwidth will open the possibility [3] of accurate timing.

Timing information can be used both to locate the source [2], or at least some of its coordinates, and to veto candidate events that are not compatible with light's speed propagation [4,5].

In order to demonstrate the practical feasibility of absolute timing with resonant antennae, we have performed an experiment with a room temperature antenna connected to our standard data analysis system [6]. The antenna is excited by a force pulse generated by a capacitive actuator, and the time of arrival of the pulse is measured by looking at the maximum of the output of the Wiener filter.

The detector has a relatively poor sensitivity as compared to cryogenic ones, but its resonant frequencies and its post detection bandwidth happen to be close to those expected for the subkelvin detectors at their sensitivity goal. As the timing accuracy depends only on these parameters, the results obtained with the present room temperature detector can be scaled directly to the subkelvin ones.

The plan of the paper is as follows in Sec. II we briefly describe the properties of signals and noise in gravitational wave (GW) resonant detectors and then, by means of the maximum likelihood approach, we give theoretical predictions for the uncertainties in the estimate of the signal amplitude and time of arrival for those detectors. Sections III

and IV are devoted to the description of the experimental apparatus and to the experimental results, respectively. Finally, in Sec. V we discuss the relevance of our results for the existing cryogenic antennae.

II. ESTIMATE OF THE TIME OF ARRIVAL

The estimate of the arrival time of a signal in the presence of Gaussian noise is a well-established problem in signal analysis [7,8]. In this section we summarize some results that are relevant for the discussion of a timing experiment with resonant detectors.

The data consist of a series of samples:

$$x_\alpha = \varepsilon_\alpha + A_0 f(t_\alpha - t_0) \quad (-N \leq \alpha \leq N), \quad (1)$$

where ε_α is the α th sample of a Gaussian, time-invariant, zero-mean stochastic process and $f(t - t_0)$ is a signal of unit amplitude arriving at time t_0 . A_0 is the "true" signal amplitude that has to be estimated together with t_0 .

In order to give an estimate for A_0 and t_0 , the method of maximum likelihood [9] searches for the minimum of the log-likelihood function,

$$\Lambda(A, t) = \sum_{\alpha, \beta = -N}^N \mu_{\alpha\beta} [x_\alpha - A f(t_\alpha - t)] [x_\beta - A f(t_\beta - t)], \quad (2)$$

as a function of A and t . In Eq. (2) the matrix $\mu_{\alpha\beta}$ is the inverse of the cross correlation matrix $\langle \varepsilon_\alpha \varepsilon_\beta \rangle = \mu_{\alpha\beta}^{-1}$, where the angular brackets indicate the mean value.

For any given t , the minimum of $\Lambda(A, t)$ is readily found at

$$\hat{A}(t) = \frac{\sum_{\alpha,\beta=-N}^N \mu_{\alpha\beta} x_{\alpha} f(t_{\beta}-t)}{\sum_{\alpha,\beta=-N}^N \mu_{\alpha\beta} f(t_{\alpha}-t) f(t_{\beta}-t)}, \quad (3)$$

with an error

$$\sigma_A^2(t) = \frac{1}{\sum_{\alpha,\beta=-N}^N \mu_{\alpha\beta} f(t_{\alpha}-t) f(t_{\beta}-t)}. \quad (4)$$

We assume from now on that, as usually happens in practice, the data span a long enough time interval so that the error in Eq. (4) is in practice independent of t : $\sigma_A^2(t) = \sigma_A^2(t_0) = \sigma_A^2$.

Equations (3) and (4) are fully equivalent to the results of the Wiener filter method, and $\hat{A}(t)$ can then be considered as the output of this filter as well.

The minimum of $\Lambda(A, t)$, at $A = \hat{A}(t)$, is given by

$$\Lambda(t) = \sum_{\alpha,\beta=-N}^N \mu_{\alpha\beta} x_{\alpha} x_{\beta} - \frac{\hat{A}^2(t)}{\sigma_A^2}. \quad (5)$$

Equation (5) shows that the best estimate for the arrival time t is the value that maximizes the signal to noise ratio:

$$\text{SNR}(t) = \left| \frac{\hat{A}(t)}{\sigma_A} \right|. \quad (6)$$

Both $\hat{A}(t)$ and $\text{SNR}(t)$ are random processes depending on the parameter t . By substituting Eq. (1) into Eq. (3) and by shifting the time axis until $t_0 = 0$, one gets that $\hat{A}(t)$ can be written as $\hat{A}(t) = A_0 R(t) + A_r(t)$. Here the function $R(t)$ is given by

$$R(t) = \frac{\sum_{i,k=-N}^N \mu_{\alpha\beta} f(t_{\alpha}-t) f(t_{\beta})}{\sum_{i,k=-N}^N \mu_{\alpha\beta} f(t_{\alpha}) f(t_{\beta})}, \quad (7)$$

while $A_r(t)$, the random part of $\hat{A}(t)$, is a zero-mean random process that, in the limit where $N \rightarrow \infty$, becomes also time invariant with autocorrelation $\langle A_r(t) A_r(t+\tau) \rangle = \sigma_A^2 R(\tau)$.

Up to linear terms in the inverse of the ‘‘true’’ signal to noise ratio $\text{SNR}_0 = A_0/\sigma_A$, $\text{SNR}^2(t)$ can then be expanded as

$$\text{SNR}^2(t) \approx \text{SNR}_0^2 \{ R^2(t) + 2R(t)[A_r(t)/A_0] \}. \quad (6')$$

Before proceeding further, it is worth pointing out that resonant detectors, both in operation or under development, consist of two or more coupled oscillators with nearby frequencies. Of these oscillators, one is the fundamental resonating mode of the detector itself and the others are provided by some form of resonant electromechanical transducers [1,2] that converts the signal into an electromagnetic one. The noise results then, at least in the neighborhood of the useful detector bandwidth, both from the narrow band noise due to excitation of those modes by different sources of random force (Brownian noise, back action noise, etc.) and from the wide band noise due to the detector read out. One can calculate [6] that in this case $R(t)$ is the superposition of few exponentially damped oscillating functions, one for each oscillator, with nearby frequencies (Fig. 1).

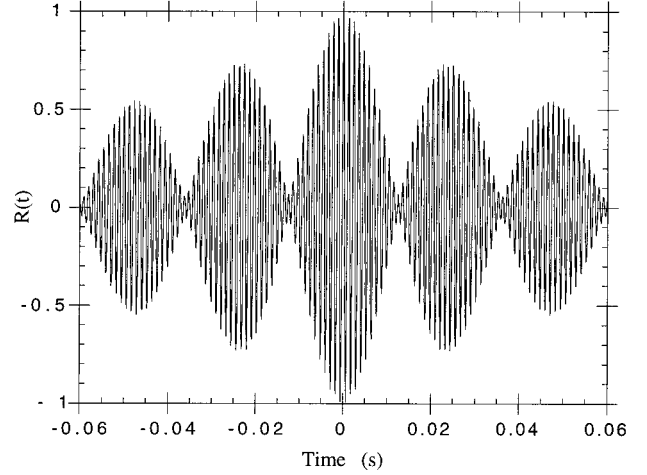


FIG. 1. Pattern of the autocorrelation function $R(t)$, with $\omega_0 = 5300$ rad/s, $\tau_0 \omega_0 = 200$, and $\omega_* = 120$ rad/s. These parameters have been measured on the room temperature antenna.

$R(t)$ shows then a series of maxima and minima approximately spaced by $T_0/2$, where $1/T_0$ is the natural frequency of the detector. The first of these extrema is always located at $t=0$.

For high enough values of SNR_0 , at each maximum of the mathematical function $R^2(t)$ corresponds a maximum of the random process $\text{SNR}^2(t)$. Because of the fluctuation of this one, the two maxima are not located at the same time value.

In the vicinity of the α th maximum of $R^2(t)$, attained at time $t = t_k$, $\text{SNR}^2(t)$ in Eq. (6') can be further expanded in powers of $t_{\phi} = t - t_k$. By truncating the expansion to second order, one can then calculate that $\text{SNR}^2(t)$ has a maximum, as a function of t_{ϕ} , at

$$t_{\phi k} = - \frac{\dot{A}_r(t_k)}{A_0 \ddot{R}(t_k)}, \quad (8)$$

where $\dot{A}_r(t_k)$ stands for the time derivative of the random process $A_r(t)$ evaluated at $t = t_k$ and $\ddot{R}(t_k)$ is the second time derivative of the function $R(t)$ at same time.

While $\ddot{R}(t_k)$ and A_0 are just numbers, $\dot{A}_r(t_k)$ is a random variable. As a consequence, $t_{\phi k}$ is also a random variable. From the standard theory of random variables one then gets, for the various mean values, that

$$\langle t_{\phi k} \rangle = - \frac{d \langle A_r(t_k) \rangle / dt}{A_0 \ddot{R}(t_k)} = 0, \quad (9a)$$

$$\langle A_r(t_k) t_{\phi k} \rangle = - \frac{\langle \dot{A}_r(t_k) A_r(t_k) \rangle}{A_0 \ddot{R}(t_k)} = \frac{\dot{R}(0)}{A_0 \ddot{R}(t_k)} = 0, \quad (9b)$$

$$\langle t_{\phi k}^2 \rangle = \frac{\langle \dot{A}_r(t_k) \dot{A}_r(t_k) \rangle}{A_0^2 \ddot{R}^2(t_k)} = - \frac{\sigma_A^2 \ddot{R}(0)}{A_0^2 \ddot{R}^2(t_k)} \approx \frac{T_0^2}{\text{SNR}_0^2 4 \pi^2 |R(t_k)|}. \quad (9c)$$

Equations (9a) and (9b) state that, within the present approximation, $t_{\phi k}$ is a zero-mean, Gaussian variable independent of $A_r(t_k)$.

Equation (9c), where the final approximate term has been obtained by using $\ddot{R}(t_k) \approx (T_0/2\pi)^2 R(t_k)$ and $R(0) = 1$, shows that the width $\sigma_{t_{\phi k}} = \sqrt{\langle t_{\phi k}^2 \rangle}$ of the Gaussian distribution of $t_{\phi k}$ is much smaller than the spacing $T_0/2$ between two adjoining maxima and is

$$\sigma_{t_{\phi k}} = \frac{T_0}{2\pi \times \text{SNR}_k}, \quad (10)$$

with $\text{SNR}_k = R(t_k)/\text{SNR}_0$ the signal to noise ratio on the k th maximum. Equation (10) is the classical formula [3] for the ‘‘phase’’ timing of narrow band signals. With this we mean that if the above timing error is converted to a phase error $\sigma_{\phi} = (2\pi/T_0)\sigma_{t_{\phi}}$, this amounts to $\sigma_{\phi k} = 1/\text{SNR}_k$.

Up to this point, then, the maximum likelihood criterion gives a discrete series of possible arrival time values $t_k \pm t_{\phi k}$, spaced roughly by $T_0/2$. For each of these possible arrival times, the estimate of the amplitude $\hat{A}(t_k)$ is a Gaussian random variable with mean value $A_0 R(t_k)$ and width σ_A . In order to get a well-defined arrival time, one has then to pick up the value t^* at which the series $|\hat{A}(t_k)|$ attains its maximum.

As already stated, for resonant detectors, $R(t)$ can be written as $R(t) = a(t)\cos(\omega_0 t) + b(t)\sin(\omega_0 t)$, with ω_0 some center ‘‘carrier’’ angular frequency not more than a few percent far from the detector resonant angular frequency $2\pi/T_0$. Here $a(t)$ and $b(t)$ are two slowly varying functions of time that consist of a combination of exponential and beating notes among the various modes of the antenna-transducer-amplifier chain. As a consequence, $R(t_k)$, which attains its maximum at $t_k = 0$ (which we assume to correspond to $k = 0$) and which is an even function of k , can be expanded, for the first few values of k , as

$$R(t_k) \approx (-1)^k (1 - |t_k|/\tau - \omega_*^2 t_k^2/2), \quad (11)$$

with τ and ω_* two constants that obey $1/\tau, \omega_* \ll \omega_0$.

In addition, as for large signal to noise ratios and for α not too large, $A_r(t_k) \ll A_0 |R(t_k)|$, then $|\hat{A}(t_k)| = |A_0 R(t_k) + A_r(t_k)| \approx A_0 |R(t_k)| + (-1)^k A_r(t_k) \equiv A_0 |R(t_k)| + A_r^*(t_k)$. It is easy to calculate that the series $A_r^*(t_k)$ has autocorrelation $\langle A_r^*(t_k) A_r^*(t_m) \rangle = \sigma_A^2 |R(t_k - t_m)|$.

The series $|\hat{A}(t_k)|$ can then be considered as made of samples of the ‘‘signal’’ $A_0 |R(t_k)|$ buried in the Gaussian zero-mean noise $A_r^*(t_k)$ and all the machinery we have applied then to extract t_{ϕ} can in principle be applied again to evaluate t^* .

If this is made, it is straightforward to calculate that the analogue of the function $R(t)$ in Eq. (7) becomes $R^*(t) \approx (1 - |t|/\tau - \omega_*^2 t^2/2)$ and two limiting case are given where quite different results are obtained.

If for all values of k in Eq. (10) $|t_k|/\tau$ is negligible in comparison to $\omega_*^2 t_k^2/2$, i.e., if $\omega_*^2 T_0 \tau/4 \gg 1$, then $R^*(t) = 1 - \omega_*^2 t^2/2$ has a well-defined second derivative at $t = 0$ and one gets that

$$\sigma_{t^*} = \frac{1}{\omega_* \times \text{SNR}_0}. \quad (12)$$

In the opposite limit where $\omega_*^2 T_0 \tau/4 \ll 1$ instead, the signal $1 - |t|/\tau$ has an infinite second derivative at the origin and the linear expansion used to get Eqs. (8) or (12) cannot be used anymore. To estimate $\sigma_{t_{\beta}}$ in this case, one can use the following argument: $|\hat{A}(t_k)|$ is approximately a Markov series. Then $|\hat{A}(t_k)| = |\hat{A}(0)|(1 - |t_k|/\tau) + \varepsilon \sigma_A \sqrt{2}|t_k|/\tau$, where ε is a zero-mean Gaussian variable with unit variance independent of $|\hat{A}(0)|$. The probability then that $|\hat{A}(t_k)| \geq |\hat{A}(0)|$ is the same as the probability that $\varepsilon \geq \text{SNR}_0 \sqrt{|t_k|/2\tau}$. The probability that $|\hat{A}(t_k)| \geq |\hat{A}(0)|$ and/or $|\hat{A}(t_{-k})| \geq |\hat{A}(0)|$ is approximately twice as much, i.e., the same as the probability that $|\varepsilon| \geq \text{SNR}_0 \sqrt{|t_k|/2\tau}$. In summary, this crude reasoning brings us to the result that t^* is approximately χ^2 distributed, with a standard deviation

$$\sigma_{t^*} = \frac{2\tau}{\text{SNR}_0^2}, \quad (13)$$

a result that can be found, based on more rigorous grounds, in Ref. [8]

As already stated, the times t_k are, within a few percent, spaced by $T_0/2$, i.e., $t_k = kT_0/2$. The random variable k has then a standard deviation

$$\sigma_k = \frac{\omega_0}{\pi \omega_* \text{SNR}_0} \left(\frac{\omega_0}{\omega_*} \right)^2 \ll \frac{\pi}{2} \tau \omega_0, \quad (14a)$$

$$\sigma_k = \frac{2\sqrt{2}\omega_0\tau}{\pi \text{SNR}_0^2} \left(\frac{\omega_0}{\omega_*} \right)^2 \gg \frac{\pi}{2} \tau \omega_0, \quad (14b)$$

and when $\sigma_k \ll 1$, the timing error reduces to the phase contribution only in Eq. (10).

In summary, the time of arrival, t , is expected to be a zero-mean random variable with an approximate distribution made of a series of Gaussian peaks with Gaussian-distributed relative amplitudes:

$$F(t) \approx \sum_{m=-\infty}^{\infty} \frac{\omega_0 \text{SNR}_m}{2\pi \sigma_k} e^{-\{[\omega_0 \text{SNR}_m (t - mT/2)]^2 + (m/\sigma_k)^2\}/2}, \quad (15)$$

where the approximation [10] has a better accuracy toward low absolute values of k .

III. EXPERIMENTAL APPARATUS AND MEASUREMENT METHODS

To experimentally test the above ideas, we have used a room temperature replica of the subkelvin AURIGA detector. The sensitive part of the apparatus is a 2.3-ton cylinder, made of 5056 aluminum alloy, suspended to a single copper wire. The fundamental mode of the antenna is at ≈ 850 Hz. A multiple-stage vibration attenuator provides, at this frequency, an attenuation of about 150 dB, which is enough to suppress the environmental noise below the thermal vibrations of the fundamental mode of the bar. The readout consists of an electromechanical capacitive, high mass transducer [2] and a very low noise (field effect transistor FET) preamplifier [11].

Briefly, the transducer consists of an aluminum disk rig-

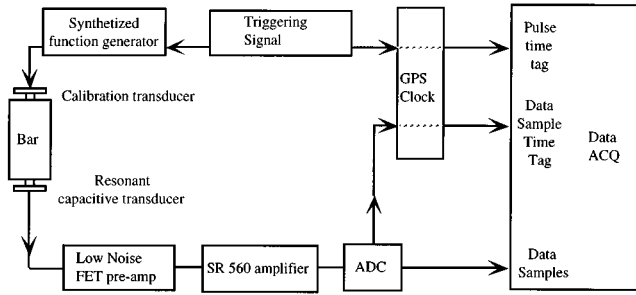


FIG. 2. Scheme of the excitation and readout systems for timing measurements. The TTL triggering signal is sent both to the synthesized function generator, which excites the bar through the calibration transducer, and to the GPS clock, which provides the time tag associate with the event. The amplified signal from the resonant capacitive transducer is digitized by the analogue to digital converter (ADC), and its samples are tagged by the same GPS clock with an accuracy of about $0.1 \mu\text{s}$.

idly connected to one of the bar end faces. The disk forms the first plate of a capacitor, the second plate of which is another disk parallel and very close to the first one ($\approx 100 \mu\text{m}$). This last disk is mechanically connected to the bar by just a thin axial rod and can thus vibrate in its first, ‘‘mushroom’’-shaped, symmetrical mode. As this mode is coupled to the oscillations of the bar, these modulate the transducer capacitance. The capacitor is charged to a charge of about $1.6 \mu\text{C}$ by means of a voltage generator, which is then disconnected. The capacitance oscillation results then in a voltage signal across the capacitor.

The signal is led to a field effect transistor (FET) preamplifier with a $12.5 \pm 0.1 \text{ G}\Omega$ input impedance and measured noise temperature and resistance of $T_n \approx 100 \text{ mK}$ and $R_n \approx 2.4 \text{ M}\Omega$, respectively [12]. The signal is further amplified by a commercial low noise amplifier.

The measurements consist of the following procedure. The bar is excited by a very short pulse of force with known amplitude and time of arrival. The resulting output signal is then collected and analyzed in order to estimate, via a suitable processing algorithm, the amplitude and time of arrival. The true and estimated values for both parameters are then compared in order to evaluate the measurement errors.

To apply the force pulse, a force actuator is mounted on the opposite side of the bar. This device is just like the transducer except that its first symmetrical mode is found at $\approx 2800 \text{ Hz}$, well above the resonant frequency of the antenna, and that the capacitor gap is wider ($200 \mu\text{m}$) than that of the transducer. The force pulse is generated by feeding on top of the dc bias, via a decoupling capacitor, a voltage signal $V(t) = V_0 e^{-t^2/\tau_0^2} \cos(\omega_0 t)$, with $\omega_0 \approx 2\pi \text{ kHz}$ and $\tau_0 \approx 1 \text{ ms}$ from a programmable signal generator. The resulting force pulse $f(t) = (E_0/C)V(t)$ thus crudely simulates the shape of the signal expected from a gravitational collapse event.

The signal generator is triggered by an external transistor-transistor logic (TTL) signal (Fig. 2), which is also sent to a GPS clock that returns the universal time (UT) to the acquisition workstation up to a precision of a few hundreds of ns. In this way we are able to tag each impulsive signal with comparable accuracy.

The amplified analog signal is then sampled at 4.9 kHz

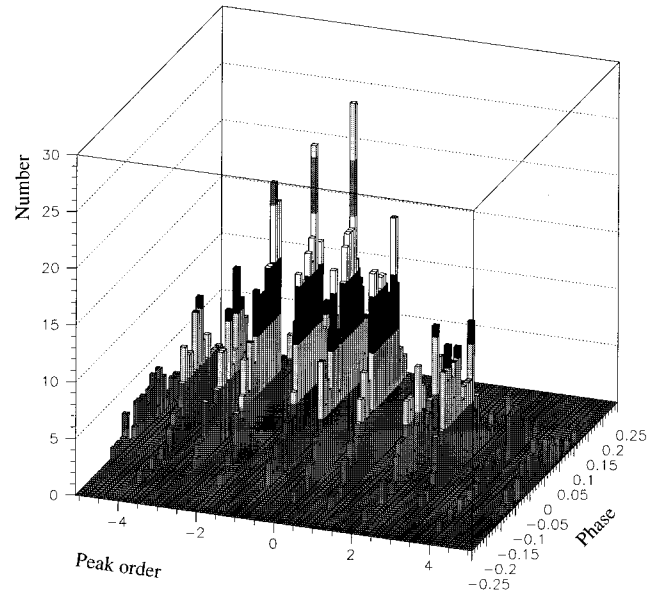


FIG. 3. Complete ‘‘peak’’ vs ‘‘phase’’ distribution of arrival times with $\text{SNR}=6$ and over 5000 trials; the ‘‘true’’ arrival time is $t=0$. The phase error is given in unit of fraction of the period $T_0 = 178 \mu\text{s}$. Notice that the phase error never exceeds $T_0/4$.

and converted into an 18 effective bit digital signal which is stored on 4.5 Gbyte magnetic tapes. Because of the presence of analog and digital filters on the acquisition line, a delay is introduced, which has been measured to be $1.976 \pm 0.001 \text{ ms}$.

The pulse arrival time is estimated by filtering data as discussed in Sec. II. Moreover, to keep track of antenna parameter drift due to slow changes of temperature and bias electric field, the Wiener filter has been made adaptive: the filter parameters (zeros and poles of the transfer function) are periodically adjusted by maximizing the signal to noise ratio of a high amplitude calibration pulse. When the maximum SNR is reached, the filter gives the correct amplitude and arrival time of any impulsive event.

For each SNR value we have collected at least a few hundreds of events. At low a SNR (i.e., $\text{SNR} \approx 6$), when measured arrival times are spread over many peaks (≥ 10), we have collected more than 5000 events.

IV. TIMING RESULTS

With reference to Fig. 1, we have separated the uncertainty in the estimate of the arrival time into the ‘‘phase error’’ t_{ϕ_k} and the ‘‘peak error’’ k by writing $\hat{t} = t_{\phi_k} + kT_*$, where k is the nearest integral value to the ratio \hat{t}/T_0 . There is no ambiguity in assigning an event to the corresponding peak order, since peaks are well separated from each other.

In Fig. 3 we show the joint histogram for ϕ_k and k for $\text{SNR}=6$. We find that within the statistical uncertainty there is no correlation between the mean and variance of t_{ϕ_k} and k at least for $k \leq 10$.

In Fig. 4 we report the standard deviation of t_{ϕ_k} for events in the central peak ($k=0$) at different SNR’s. The solid line represents the fit to the experimental data of the power law

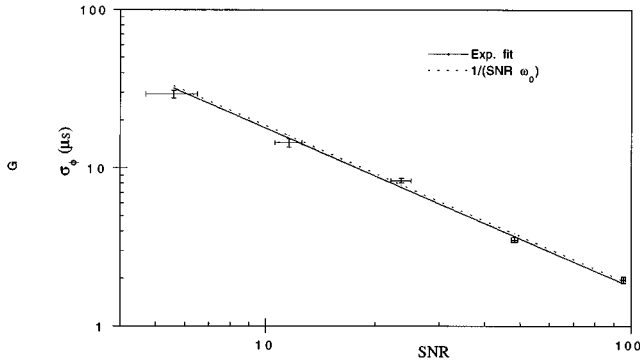


FIG. 4. Fit to the experimental data (solid line) and theoretical (dotted line) curve of the “phase” standard deviation σ_ϕ as a function of the SNR. The experimental points refer to the central peak events.

P/SNR , from which we obtain $P = 178 \pm 3 \mu\text{s}$. This value has to be compared with $1/\omega_0 = 185 \mu\text{s}$.

In Fig. 5 we report the histogram of the distribution of k , which is just the projection of the bidimensional histogram of Fig. 3 over the k axis. Again, those data refer to $\text{SNR} = 6$.

In Fig. 6 we plot the standard deviation σ_k of k as a function of the SNR. The error bar associated with each data point of Fig. 6 has been estimated as follows. For $\text{SNR} \leq 10$, k is spread over many integer values and the standard Gaussian estimator of the variance is a reasonable choice. In this case the variance of the estimate has a relative error $\approx \sqrt{(2/N)}$, where N_e is the total number of events in the histogram.

At a high SNR (> 10), most of the events fall into the central peak, which gives no contribution to the estimate of the variance, and hence the error on the latter must be much higher than the Gaussian estimate. Assuming a Poisson dis-

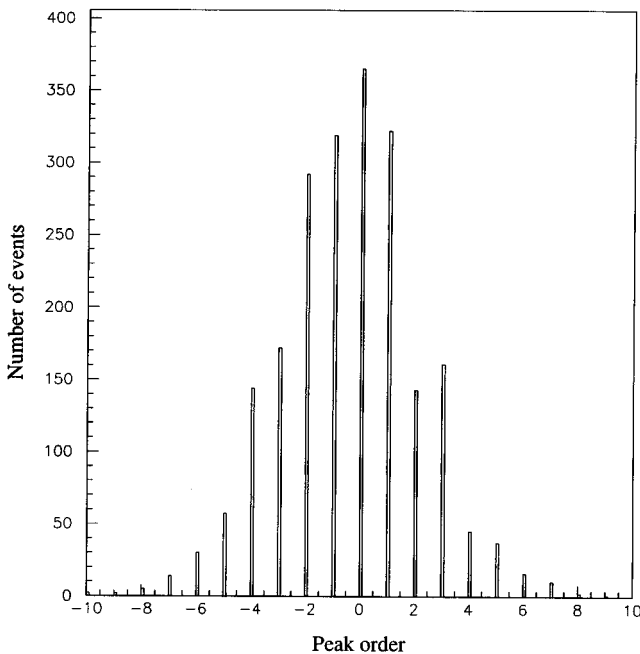


FIG. 5. “Peak” distribution of the arrival times obtained with $\text{SNR} = 6$.

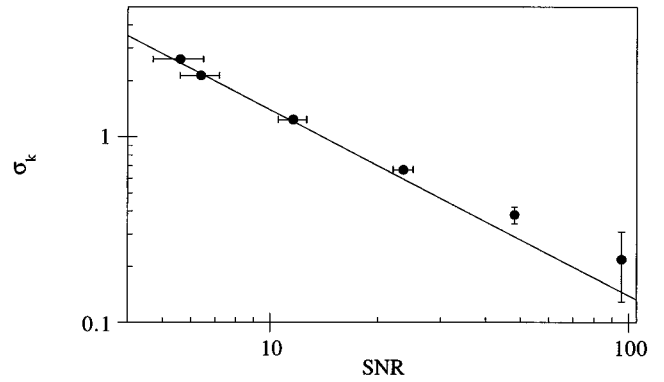


FIG. 6. Experimental (●) and theoretical (line) values of the “peak” error as a function of the SNR. If $\sigma_k \leq 1$ (i.e., $\text{SNR} > 20$), the total uncertainty of the arrival time reduces to the phase contribution of Fig. 3. The line represents the theoretical prediction of Eq. (14a).

tribution for the rare events falling outside the central peak, we calculate that the relative error on σ_k is of the order of $1/\sqrt{N_e - N_{e0}}$, where N_{e0} is the number of events with $k = 0$.

V. CONCLUSIONS

The experimental results obtained above support quantitatively the standard theory presented in Sec. I. To be specific the result show that (1) t_{ϕ_k} is independent of k , (2) that Eq. (10) for the phase noise is obeyed, and (3) that for the kind of “one beat note” autocorrelation function we achieved with our room temperature antenna Eqs. (14) hold. It must be noted that the room temperature detector parameters were found [13] to be $\omega_* \approx 120 \text{ rad/s}$ and $\tau_0 \approx 75 \text{ ms}$. Here τ_0 is the decay time of the two exponentials that enters in $R(t)$. However, the parameter τ in Eq. (11) is a complicated function of ω_* and τ_0 and one can estimate that in our case $\tau \gg \tau_0$ so that we are fully in the regime of Eq. (14a), $\omega_*^2 T_0 \tau / 4 > 1$. It can be seen from Fig. 6 that experimental data indeed reasonably fit the theoretical behaviour of σ_k vs SNR predicted by Eq. (14a), the slight, barely significant excess of experimental data with respect to the theoretical curve, being fully accounted for by the imperfections of the filter mask.

The overall timing ability of the room temperature antenna is then such that for $\text{SNR} > 20$ the total uncertainty on the arrival time is $\sigma_t \approx 174 \mu\text{s}/\text{SNR}$.

Being the antenna in the regime of Eq. (14a), the uncertainty is mainly dominated by the nonoptimal matching of the transducer to the antenna itself and to a comparatively poor performance of our FET amplifier as compared, for instance, to a superconducting quantum interference device (SQUID) one. All this brings a comparatively low value for ω_* .

The transducer used in the present experiment has been indeed optimized to work at low temperature with a low noise SQUID amplifier. Matching to those conditions yielded a mass of $M = 2.17 \text{ kg}$ and an unperturbed frequency value for the transducer of $\nu = 875 \text{ Hz}$ at room temperature. An optimal choice for the room temperature detector would have yielded a much lower value for the mass, M

≈ 0.05 kg. This detuning is the source of the above-mentioned limitation.

When the same transducer is assembled on AURIGA and if a SQUID noise performance corresponding to a noise energy density per unit frequency of $e \approx 100\hbar$ is attained, the detector will have $\omega_* \approx 200$ rad/s. This will give the same timing performance as that achieved above, but for $\text{SNR} > 12$.

We believe that the main result of our test is the prospects it opens for the near future, when different kinds of detectors will be operating together. For the class of impulsive gravitational signals (SN explosions, to give an example) without a characteristic waveform pattern, comparison between different detectors is the only way to reject fake events and gain information on the signal, and accurate timing on each of them is the *conditio sine qua non*.

At the moment five resonant bars are operating worldwide, so that simple triangulation can be performed to determine the source position by measuring time-of-flight delays between different detectors. The timing precision we have reached is sufficient to apply this method even at regional

scales, as for the Italian gravitational wave detectors AURIGA, NAUTILUS, and VIRGO.

High precision absolute timing, however, opens the way to a more accurate method of analysis of gravitational signals. In fact, it has been shown [2] that with at least six resonant bars one can reconstruct on the same wave front the amplitude and direction of propagation of the wave, in order to solve “the inverse problem” and test the Riemann tensor’s transversality and tracelessness. Source position can also be determined within few arcmin. This method can be easily extended to the upcoming global network of bars (AURIGA, NAUTILUS) and interferometers [(TAMA 300, GEO 600, Laser Interferometric Gravitational Wave Observatory (LIGO), VIRGO)], which all are expected to have the same sensitivity at 1 kHz and will thus provide the first actual gravitational wave observatory.

In addition, correlation between instruments operating on different physical principles, such as resonant bars and interferometers, is very important not only because it provides a way to compare independently generated data, but also because different detectors have different noise sources and hence spuria rejection will be much more reliable.

-
- [1] See, for instance, M. Cerdonio, P. Falferi, G. A. Prodi, A. Ortolan, S. Vitale, and J. P. Zendri, *Physica B* **194**, 3 (1994); M. Cerdonio, G. A. Prodi, A. Ortolan, S. Vitale, and J. P. Zendri, in *TAUP 93*, Proceedings of the Third International Workshop on Theoretical and Phenomenological Aspects of Underground Physics, Assergi, Italy, 1993, edited by C. Arpesella *et al.* [*Nucl. Phys. B (Proc. Suppl.)* **35**, 75 (1994)].
- [2] AURIGA at Legnaro INFN National Laboratories, see M. Cerdonio *et al.*, in *Proceedings of the First Edoardo Amaldi Conference on Gravitational Wave Experiments*, edited by E. Coccia, G. Pizzella, and F. Ronga (World Scientific, Singapore, 1995), p. 176; Nautilus at Frascati INFN National Laboratories, see P. Astone *et al.*, in *ibid.*, p. 161.
- [3] M. Cerdonio, P. Fortini, G. A. Prodi, A. Ortolan, and S. Vitale, *Phys. Rev. Lett.* **71**, 4107 (1993).
- [4] S. Vitale, G. A. Prodi, J. P. Zendri, A. Ortolan, L. Taffarello, G. Vedovato, M. Cerdonio, and D. Pascoli, in *Proceedings of the International Conference on “Gravitational Waves, Sources and Detectors,”* edited by F. Fiduciaro and I. Ciufolini (World Scientific, Singapore, 1997), p. 256.
- [5] A. Ortolan, Ph.D. thesis, University of Ferrara, 1992, M. Cerdonio, P. Fortini, A. Ortolan, and S. Vitale, in *Proceedings of the 10th Italian Conference on General Relativity and Gravitational Physics*, edited by M. Cerdonio, R. D’Auria, M. Francaviglia, and G. Magnano (World Scientific, Singapore, 1994), p. 111.
- [6] A. Ortolan, G. Vedovato, M. Cerdonio, and S. Vitale, *Phys. Rev. D* **50**, 4737 (1994); S. Vitale *et al.*, in *Proceedings of the First Edoardo Amaldi Conference on Gravitational Wave Experiments* [2], p. 220.
- [7] J. A. Lobo, *Mon. Not. R. Astron. Soc.* **247**, 573 (1990).
- [8] P. Swerling, *J. Soc. Ind. Appl. Math.* **7**, 152 (1959), and references therein.
- [9] See, for instance, C. W. Helstrom, *Statistical Theory of Signal Detection* (Pergamon, Oxford, 1968).
- [10] $F(t)$ is even normalized in an approximated way.
- [11] D. Carlesso, Ph.D. thesis, University of Padua, 1996.
- [12] Stanford Research SR560 FET amplifier.
- [13] V. Crivelli-Visconti, Ph.D. thesis, University of Rome “la Sapienza,” 1996.